Hypoxic Rise in Cytosolic Calcium and Renal Proximal Tubule Injury Mediated by a Nickel-Sensitive Pathway

M. BARAC-NIETO,† A. CONSTANTINESCU,‡ M. H. PINA-BENABOU,* AND R. ROZENTAL*,[1]

Department of Cell Biology and Anatomy and Departments of Obstetrics and Anesthesiology, New York Medical College, Valhalla, New York 10595; †Department of Physiology, Kuwait University, Kuwait; and ‡Children's Hospital, Hollywood, Florida 33021

In the kidney, cell injury resulting from ischemia and hypoxia is thought to be due, in part, to increased cytosolic Ca^{2+} levels, $[Ca^{2+}]i$, leading to activation of lytic enzymes, cell dysfunction, and necrosis. We report evidence of a progressive and exponential increase in $[Ca^{2+}]i$ (from 245 ± 10 to 975 ± 100 n*M* at 45 mins), cell permeabilization and propidium iodide (PI) staining of the nucleus, and partial loss of cell transport functions such as Na^+-gradient–dependent uptakes of ^{14}C-alpha-methylglucopyranoside and inorganic phosphate (^{32}Pi) in proximal convoluted tubules of adult rabbits subjected to hypoxia. The rise in $[Ca^{2+}]i$ depended on the presence of extracellular $[Ca^{2+}]$ and could be blocked by 50 μ*M* Ni^{2+} but not by verapamil (100 μ*M*). Presence of 50 μ*M* Ni^{2+} also reduced the hypoxia-induced morphological and functional injuries. We also used HEK 293 cells, a kidney cell line, incubated in media without glucose and exposed for 3.5 hrs to 1% O_2–5% CO_2 and then returned to glucose-containing media for another 3.5 hrs in an air–5% CO_2 atmosphere and finally exposed for 1 min to media containing 1 μ*M* PI. $NiCl_2$ (50 μ*M*) or pentobarbital (300 μ*M*) more than phenobarbital (1.5 m*M*), when present in the incubation medium during both the hypoxic and the reoxygenation periods, induced significant ($P < 0.001$) reductions in the number of cell nuclei stained with PI, similar to their relative potency as inhibitors of T channels. Our findings indicate that hypoxia-induced alterations in calcium level and subsequent cell injury in the proximal convoluted tubule and in HEK cells involve a nickel-sensitive and dihydropyridine insensitive pathway or channel. Exp Biol Med 229:1162–1168, 2004

This work was supported in part by grants from Kuwait University Research Administration (M.B.N.), the National Institutes of Health (R.R.), the Epilepsy Foundation (R.R.), and Millenium Institute for Tissue Bioengineering (CNPq) and by a training fellowship grant from the National Institutes of Health (DK07110-19) (A.C.).

[1] To whom correspondence should be addressed at Department of Cell Biology and Anatomy, BSB Room A21, Departments of Obstetrics and Anesthesiology, New York Medical College, Valhalla, NY 10595. E-mail: r_rozental@nymc.edu

Received May 10, 2004.
Accepted September 14, 2004.

1535-3702/04/22911-1162$15.00

Key words: hypoxia; calcium; nickel; kidney; HEK cells; pentobarbital; phenobarbital

Introduction

Acute renal failure is a common and serious consequence of hypoxic episodes that occurs as a result of trauma, burns, surgery, or kidney transplantation. Degrees of susceptibility to hypoxic injury depend on a number of factors, including the availability of anaerobic energy (1, 2), energy demands (3), the ability to maintain cell integrity (4), and the extent of oxidative cell injury associated with reoxygenation (5).

Increase in cytosolic Ca^{2+} levels, $[Ca^{2+}]i$, subsequent to a hypoxic insult has been suggested to play an important role in excitotoxic cascades leading to cell injury (4, 6, 7). In excitable tissues, voltage- and ligand-gated channels appear to be involved in the $[Ca^{2+}]i$ increase during ischemia or hypoxia (8). A similar mechanism has been suggested to be present in the kidneys (9, 10).

Expression of voltage-gated Ca^{2+} channels of L, N, and P types has been documented in kidneys vasculature but not in the proximal tubules (11, 12). These channels appear to be involved in the rise in cell calcium associated with renal injuries. Although clinical use of compounds such as dihydropyridines (e.g., verapamil) to block channels and prevent acute renal failure (13) has been advocated, the nature of channels with a pivotal role in mediating Ca^{2+} influx in hypoxic proximal convoluted tubules (PCTs) is not well understood. Recent works suggest involvement of other pathways. This is supported by presence of, for example, stretch-activated nonspecific cationic channels in the luminal membrane of *Necturus* PCT capable of mediating Ca^{2+} currents during cell swelling (14) or the presence of nifedipine-sensitive cation channels (15).

Recently, novel types of Ca^{2+} antagonists have been developed. Blockade of T-type channel particularly through the inhibition of intracellular Ca^{2+} release has been effective in treating a variety of reveal diseases (16). The most ubiquitous T-type Ca^{2+} channel is the $Ca_v3.2$ channel,

which is expressed in several tissues, among them the kidney (17). Of particular interest, barbiturates block T-type Ca^{2+} channels in concentrations that occur in clinical practice. In HEK 293 cells, their ability to block $Ca_v3.1$ channels falls into the following order: pentobarbital (310 μM) > phenobarbital (1.5 mM).

In this report, we present evidence for a pathway involved in progressive exponential increases in $[Ca^{2+}]i$ levels, dysfunction of PCTs, and tubule cell injury induced by *in vitro* anoxia and sensitive to micromolar concentrations of $NiCl_2$ but not to verapamil. In a kidney cell line, $NiCl_2$, pentobarbital, and phenobarbital protected against hypoxia induced cell permeabilization with the same relative potency they exhibit as inhibitors of T-type calcium channels. Work is underway to identify the channel or molecules responsible for these observations.

Materials and Methods

Animals. Adult female New Zealand White rabbits used in this study were obtained from Hazelton Dutchland Farms (Denver, PA) and Charles River (Quebec, Canada).

Tubules. Rabbits were euthanized by an intraperitoneal administration of 100 mg/kg pentobarbital. Kidneys were removed through a midline incision and placed in chilled HEPES-buffered Ringer's-like solution containing (in mM) 137 NaCl, 1.2 $MgSO_4$, 2.5 K_2HPO_4, 2 $CaCl_2$, 5 HEPES, 5.5 glucose, 5 lactate, and 6 alanine. Kidneys were decapsulated and coronal slices were obtained. S1 and S2 PCT segments were microdissected free-hand in chilled Ringer's-like solution from the kidney cortex slices. Tubule segments were mounted to precooled 0.5 x 2-mm glass coverslips coated with Cell-Tak (Collaborative Biomedical Products, Bedford, MA). The length of the segments (~0.75 mm) was measured with an optical micrometer (Leica, Buffalo, NY).

Anoxia. For anoxic exposure, the coverslips were submerged in bicarbonate (25 mM)-buffered Ringer's-like solution (in mM: 137 NaCl, 1.2 $MgSO_4$, 2.5 K_2HPO_4, 2 $CaCl_2$, 5.5 glucose, 5 lactate, and 6 alanine) in an air-tight chamber (9) gassed with a mixture of 95% N_2–5% CO_2 at 37°C. For oxygenation, a gas mixture of 95% O_2–5% CO_2 was used.

Intracellular Ca^{2+} ($[Ca^{2+}]i$). Tubules were loaded with 10 mM fura-2 AM (Molecular Probes Inc., Eugene, OR) by incubation in HEPES-buffered metabolite containing Ringers's-like solution for 60 mins at 37°C. Tubules were then superfused in an air-tight chamber with a similar solution buffered with 25 mM bicarbonate and gassed either with 95% O_2 or 95% N_2 and 5% CO_2 at 37°C for 30 mins on a thermostated stage of an inverted microscope (Zeiss Axiovert 35M, Göttingen, Germany). $[Ca^{2+}]i$ images were obtained with a charge-couple device camera (Quantex Co., Sunnyvale, CA) and were digitized at excitation wavelengths of 340 and 380 nm with a filter wheel (American Precision, Oceanside, CA) with emission set above 480 nm by a dichroic mirror. Data were analyzed by Image 1AT/FL software (Universal, Media, PA). The pixel arrays were 580 x 320 mm, and pixel-by-pixel ratio imaging was used to obtain spatial maps of $[Ca^{2+}]i$ distribution in images of single tubules. Background levels were subtracted and the intensity ratios of individual pixels were calculated through logarithmic subtraction as previously described (18, 19). Averages of four map images at each wavelength were used to obtain the ratio of 380:340 for the images. Values of $[Ca^{2+}]i$ levels were calculated by the dissociation constant (225 nM) for Ca^{2+}-fura-2 at 37°C (20). $[Ca^{2+}]i$ levels were measured in different experimental conditions. Bathing solution contained either 0 or 2 mM $[Ca^{2+}]$. Concentration of the mitochondrial proton uncoupler carbonyl-cyanide-trifluoromethoxy-phenylhydrazone (FCCP) in the perfusion medium was kept at 5 mM. Ringer's-like solution containing 100 mM potassium chloride (KCl) was used to study the role of voltage-dependent channels.

Functional Assay. Kidneys were removed from euthanized rabbits 10 mins after the rabbits received 20 ml/kg iv of a warm solution containing isotonic sucrose and 2% Agarose #IX (Sigma Chemical Co., St. Louis, MO). Proximal tubules with open lumen were microdissected and mounted onto coverslips as described above. Slides were then bathed in bicarbonate buffered Ringers's-like solution gassed with either 95% N_2 or 95% O_2 + 5% CO_2 at 37°C for 1 hr. Slides were reoxygenated for 15 mins in bicarbonate-buffered Ringers-like solution in 95% O_2–5% CO_2 at 37°C, and alpha-methyl-glucopyranoside (AMG) labeled with 0.1mM ^{14}C-labeled and 0.1mM ^{32}Pi (inorganic phosphorus) were added to the incubation solution for the next 15 mins. ^{32}Pi and AMG glucose uptakes were allowed to proceed for 15 mins. The tubules were then washed three times with ice-cold isotope-free incubation solution 10 ml at a time. Radioactivity was measured immersing coverslips in scintillation liquid in a Wallac model 1400 liquid scintillation counter (Wallac Oy, Turku, Finland). Uptake data were expressed as the ratios of radioactivity found in hypoxic to those in control tubules.

Membrane Integrity. Membrane integrity was estimated by nuclear staining for 1 min in a Ringer's-like solution containing 5 mg/ml propidium iodide (PI). The intensity of staining was measured by fluorescence microscopy (21) with an inverted Nikon epifluorescence microscope equipped with a Xenon lamp, a 495-nm excitation filter, and a ×10 objective after the slides were washed three times with phosphate-buffered saline (PBS) and fixed with 4% paraformaldehyde in PBS. The emitted light above 580 nm was collected with a dichroic mirror, filtered at 620 nm, and magnified with a ×2 lens.

Tubule Images. Images of formaldehyde-fixed microdissected segments were obtained by differential interference contrast with Nikon optics (×60 panaplo, numerical aperture 1.4, differential interference contrast objective). Images were processed on an 80286 personal computer and

a Newvicon high-resolution video camera. Images were printed at a magnification of ×2500.

HEK 293 cells (ATCC; Global Bioresource Center, Manassas, VA), a kidney cell line previously used to evaluate the effects of several agents on expressed Ca^{2+} channels (17, 22, 23), were also used. Cells were grown to confluence in Dulbecco's modified Eagle's medium supplemented with fetal bovine serum (10%) and antibiotics (1%) (Cellgro; Fisher Scientific, Pittsburgh, PA) on 35-mm petri dishes. Then the cells were incubated in media without glucose (Krebs-Henseleit buffer) (24) containing (in m*M*) 115 NaCl, 3.6 KCl, 1.3 KH_2PO_4, and 25 $NaHCO_3$ and exposed for 3.5 hrs (5-hr exposure to these conditions resulted in irreversible deaf of almost 100% of the cells) to 1% O_2–5% CO_2 (Thermo Forma Incubator, Marietta, OH). The cells were returned to glucose-containing media for another 3.5 hrs in air–5% CO_2 and were finally exposed for 1 min to media containing 1 μ*M* PI.

Statistics. Values are expressed as mean ± SEM. The number of tubules from different animals is shown by *n*. Analysis of variance followed by two-tailed Student's *t* test or Dunn multiple-comparison nonparametric test was used to assess statistical significance ($P < 0.05$).

Results

Effect of Hypoxia on the Levels of $[Ca^{2+}]i$ in Isolated PCTs. Exposure to a mixture of 95% N_2–5% CO_2 (Fig. 1) leads to progressive increases in $[Ca^{2+}]i$ in S1 segment cells from <180 n*M* (blue) to <450 n*M* (yellow) to <600 n*M* (red) and to >650 n*M* (white) during a period of 45 mins (Fig. 1). In most tubules studied ($n = 10$) the increase occurs exponentially and homogeneously throughout the

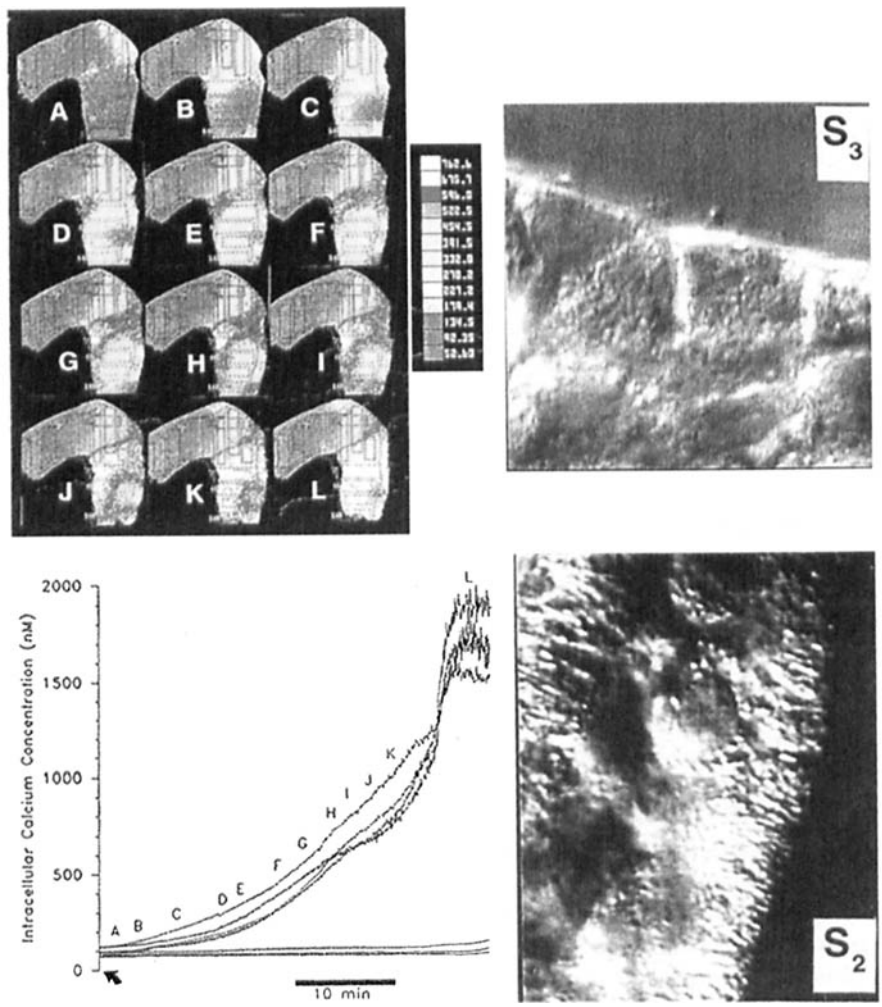

Figure 1. Hypoxia-induced $[Ca^{2+}]i$ increase in proximal convoluted tubule from an adult rabbit. Pseudocolor images of $[Ca^{2+}]i$ levels in a tubule treated with 100 μ*M* verapamil (Top). Images A–L were taken at 5-min intervals after initiation of perfusion with media gassed with a mixture of 95% N_2–5% CO_2. Note the progressive change in $[Ca^{2+}]i$, starting at the center of the segment and extending in a unidirectional manner, from blue (<180 n*M*) to yellow (< 450 n*M*) to red (< 600 n*M*) to white (>650 n*M*). Changes in $[Ca^{2+}]i$ levels as a function of time for different proximal convoluted tubule regions over the same time period illustrated in A–L (Bottom). Differential interference contrast microscopic images of the same proximal tubule where $[Ca^{2+}]i$ were measured (×2500) are also shown. In S3, the basal cell membranes were smooth (Top right) and $[Ca^{2+}]i$ remained low throughout the hypoxic period. In S2 (Bottom right) were pronounced basal infoldings, and $[Ca^{2+}]i$ progressively increased during hypoxia.

microdissected segment. In a few proximal tubules (n = 3), such as the segment shown in Figure 1, the exponential elevation in $[Ca^{2+}]i$ began at the center from a homogeneous low level and spread only toward S2. The center corresponded to a transition from S2-type cells with pronounced basolateral invaginations of the cell membrane to S3-type cells exhibiting a smooth basal cell membrane (Fig. 1, right panels). In S3 segment cells, levels of $[Ca^{2+}]I$ were 260 ± 25 n*M* after 30 mins of hypoxia (eight different tubules).

The increase in proximal tubule $[Ca^{2+}]i$ induced by 95% N_2–5% CO_2 (Table 1) was not sensitive to 100 μ*M* verapamil but could be reduced by removing the extracellular $[Ca^{2+}]o$ or 50 μ*M* $NiCl_2$ (Table 1). Hyperosmotic perfusate containing 100 m*M* KCl produced a very rapid (<1 min) and transient increase in $[Ca^{2+}]i$ throughout the PCT (Table 1). This rise was sensitive to Ni^{2+} and was reduced to 256 n*M* by 50 μ*M* NiCl2. Presence of 5 μ*M* FCCP induced a large increment in $[Ca^{2+}]i$, which was also blocked by 50 μ*M* NiCl2 (Table 1).The rapid rise in $[Ca^{2+}]i$ did not occur in the presence of 200 m*M* mannitol in the perfusate.

Tubule Transport Functions. Sodium gradient-dependent uptake of AMG occurs exclusively via luminal Na^+-dependent glucose co-transporters, whereas uptake of Pi can be mediated by luminal as well as by basolateral co-transporters. The uptake of these two solutes decreased to 20% and 50% of controls, respectively, after 30 mins of anoxia followed by 30 mins of reoxygenation. Changes in the transport rates of AMG or Pi were minimized, but not fully alleviated, by exposure to 50 μ*M* $NiCl_2$ during the hypoxic period (Fig. 2). $NiCl_2$ (50 μ*M*) had no effect on AMG or Pi uptakes (ratios of uptakes by Ni treated to untreated equaled 1.02 ± 0.1 and 0.98 ± 0.2, n = 6, respectively) in tubules maintained in 95% O_2–5% CO_2.

Cell Permeability to Propidium Iodide During

Table 1. Levels of Cytosolic Ca^{2+} in Proximal Convoluted Tubules of Mature Rabbits (n*M*)[a]

	Control	Hpoxia
Control	245 ± 10	975 ± 100
+$[Ca^{2+}]_o$ = 0	90 ± 6	158 ± 20
+100 μ*M* verapamil	240 ± 20	850 ± 160
+50 μ*M* $NiCl_2$	295 ± 10	287 ± 12
+100 m*M* KCl	920 ± 90	—
50 μ*M* $NiCl_2$ + 100 m*M* KCl	256 ± 9	—
+ 5 m*M* FCCP	910 ± 83	—
5 m*M* FCCP + 50 μ*M* $NiCl_2$	290 ± 80	—

[a] Exposure to nominally Ca^{2+}-free solution ($[Ca^{2+}]_o$ = 0), verapamil, and $NiCl_2$ was continuous during the hypoxic period (45 mins in 95% N_2–5% CO_2). Potassium chloride was added at the final concentration indicated and washed out during aerobic perfusion at 1 ml/min. No effect of an isosmotic amount of mannitol (200 m*M*) on $[Ca^{2+}]i$ was noted. Beyond 45 mins of hypoxia, measurements became unreliable because of leakage of the indicator and saturation of the remaining Fura-2. Maximal $[Ca^{2+}]_i$ measurable in each experimental condition are tabulated. Data are mean ± SEM of repeated measurements in three to eight different tubules. KCl, potassium chloride; FCCP, carbonyl-cyanide-trifluoromethoxy-phenylhydrazone.

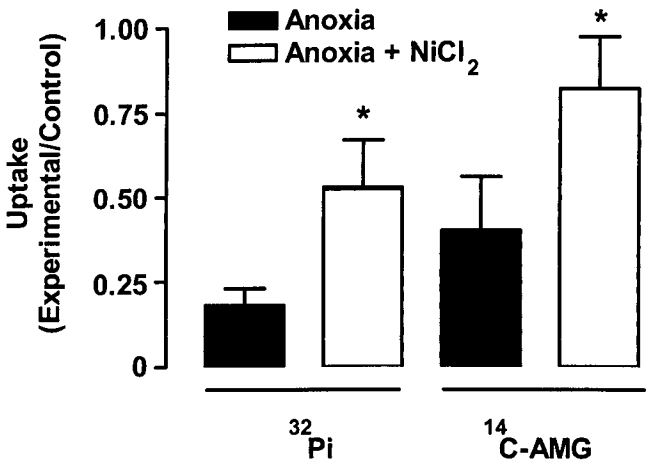

Figure 2. Changes in the tubule cell uptake. Changes in uptake of alpha-methyl-glucopyranoside or inorganic phosphate (P_i) observed in proximal convoluted tubules exposed for 30 mins to 95% N_2–5% CO_2 (hypoxia) in the presence (n = 6) or absence (n = 7) of 50 μ*M* Ni^{2+} followed by recovery in 95% O_2–5% CO_2 for 30 mins. Controls were continuously exposed to 95% O_2–5% CO_2. Data are presented as mean ± SE. AMG, alpha-methyl-glucopyranoside. * $P < 0.05$.

Anoxia. A large number of PCT cells lost cell membrane impermeability to PI when exposed to anoxia. In fact, 85% ± 2% of these cells (n = 4 tubules) showed PI nuclear staining when maintained in 95% N_2–5% CO_2 for 60 mins (Fig. 3A). However only 10% ± 4% showed nuclear staining (n = 5 tubules) when 50 μ*M* $NiCl_2$ was present during the anoxic period (Fig. 3B).

In HEK cells, exposure to 3.5-hr hypoxia induced substantial (about 50%) cell death, as indicated by PI staining. $NiCl_2$ (50 μ*M*) or pentobarbital (300 μ*M*) more than phenobarbital (1.5 m*M*), when present in the incubation medium during both the hypoxic and the reoxygenation periods, conferred substantial protection, as reflected by

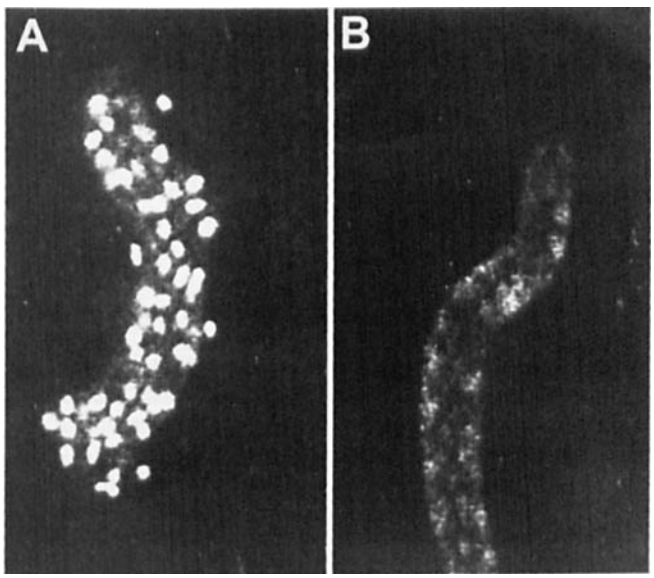

Figure 3. Nuclear staining with propidium iodide of proximal convoluted tubule segments exposed to 95% N_2–5% CO_2 for 60 mins in the absence (A) or presence (B) of 50 μ*M* $NiCl_2$.

significant reductions in the number of cell nuclei stained with PI per 1.08 mm^2 field (Table 2). Of particular interest to this study, $NiCl_2$, pentobarbital, and phenobarbital have similar relative potencies as inhibitors of the T-type Ca_v3 channels expressed in HEK cells (17).

Discussion

Hypoxia Induces $[Ca^{2+}]I$ increase. Earlier works by Weinberg *et al.* (4) and Kribben *et al.* (9) have shown that hypoxia can increase $[Ca^{2+}]i$ levels by 2-fold in rat proximal tubules within 5 mins and before any significant cell damage. These reports have also shown that leakage of the indicator dye from PCTs does not interfere with $[Ca^{2+}]i$ measurement during the first ~45 mins of the hypoxic period. The protective effect of BAPTA[1,2-bis(2-amino-phenoxy)-ethane-N,N,N′,N′-tetraacetic acid], used as an intracellular Ca^{2+} buffer, supports a role for high $[Ca^{2+}]i$ in the initiation of hypoxic injury in proximal tubule (9). This is in contrast to the findings in collagenase-treated suspensions of proximal tubules where no significant change was observed in cytosolic-free $[Ca^{2+}]i$ with hypoxia (25). This may be due to the predominance of S3 segments (25) or of tubules from very young animals (26), which are more resistant to hypoxic insults. Moreover, continuous tubule superfusion may wash out substances released into the medium, which may minimize $[Ca^{2+}]i$ changes in the tubule. Here, we report a 3- to 4-fold increase (from <200 to >600 n*M*) in $[Ca^{2+}]i$ in most of the proximal tubule cells during the first 30 mins of anoxia. In segments such as the ones shown in Figure 1, $[Ca^{2+}]i$ was initially measured to be at 100 n*M* throughout tubule before hypoxic insult. The $[Ca^{2+}]i$ level began to progressively increase at the center of the segment, spreading in only one direction. Cells localized in S2 to S3 segments with different tolerance to hypoxia may be responsible for such localized changes in $[Ca^{2+}]i$. It has already been documented that cells with a smoother basolateral cell membrane, localized in S3, are more tolerant to *in vitro* hypoxia and are more glycolytic than S2 cells (1). Inhibition of aerobic metabolism may also explain the $[Ca^{2+}]i$ increase that occurs when ATP is depleted in the presence of the mitochondrial uncoupler FCCP (Table 1).

The hypoxia-induced increase in $[Ca^{2+}]i$ could be partly prevented by removing $[Ca^{2+}]o$ or by 50 μ*M* $NiCl_2$. This suggests that Ca^{2+} influx is more important in the elevation of cytosolic $[Ca^{2+}]i$ when ATP is reduced than are other mechanisms of Ca^{2+} level control, such as inhibition of Ca^{2+} extrusion or active Ca^{2+} accumulation in the endoplasmic reticulum. $NiCl_2$ may contribute to Ca^{2+} level homeostasis by inhibiting other ATP-requiring processes and shunting ATP to fuel the calcium pumps. Continuous operation of the active calcium transport machinery may prevent pronounced rises in $[Ca^{2+}]i$. However, $NiCl_2$ does not appear to have a significant effect on the activity of Na-K ATPase, which is central to actively maintain cell Na^+ and K^+ gradients. This is indicated by the facts that $NiCl_2$ did not alter the Na^+ gradient-dependent uptakes of Pi or of AMG in PCTs incubated aerobically and stimulated rather than inhibited recovery of Na^+ gradient-dependent uptakes of Pi and AMG and of cytosolic calcium after anoxia and reoxygenation. Moreover, it is not likely that $NiCl_2$ may have caused a reversal of intracellular Ca^{2+} for extracellular Na^+ exchange, which could also contribute to the observed rise in $[Ca^{2+}]I$. Such reversal requires much higher $NiCl_2$ concentration than the micromolar level used in these experiments (27).

Rapid depolarization of the renal tubule cells by transient increases in extracellular $[K^+]$ also resulted in increases in $[Ca^{2+}]I$. Although the anoxic rise could be of the same magnitude (5- to 10-fold), it requires more time to occur (30 mins). However, this effect of KCl supports the existence of voltage-sensitive Ca^{2+} entry pathways in proximal tubule cells (14, 28).

Moreover, in proximal tubules $[Ca^{2+}]i$ increases induced by olvanil (a vanilloid agonist) were prevented by removal of extracellular Ca^{2+} or by La^{3+} but not by dihydroxypyridines, verapamil, or diltiazem (29). L-type, dihydropyridine-sensitive, high-voltage activated channels are expressed in distal nephron segments and in the renal vasculature, whereas epithelial-type calcium channels, CaT1 (TRPV6) and ECaC (TRPV5), have been found in the renal distal tubules where they mediate hormone-regulated Ca^{2+} reabsorption (30, 31). These channels have not been found in renal PCTs. Moreover, luminal, nifedipine-sensitive cation channels in proximal straight (S3) segments (15) are apparently not responsible for the changes in $[Ca^{2+}]i$ documented here, for S3 (straight) segments are not sensitive to hypoxia. Thus, it appears that different Ca^{2+} pathways function in the various segments of the proximal, in the distal nephron, and in vascular structures. Such differences may account for the different susceptibilities of these structures to the hypoxia-induced $[Ca^{2+}]i$ rise and subsequent injury and may at least, in part, explain the partial protective effect of dihydropyridines in acute renal failure (13). Surprisingly, verapamil was not able to block the PCT pathway, which was instead inhibited by $NiCl_2$, a T-type channels blocker. These findings, hence, provide support for the involvement of low-voltage–activated T-type channels in the regulation of cell Ca^{2+} in S1 and S2 cells of the proximal tubules. Indeed, the existence of such channels has been recently documented in rabbit renal proximal

Table 2. $NiCl_2$, Pentobarbital, and Phenobarbital Protect HEK Cells Against Hypoxic Insults. Number of Propidium Iodide–Positive Cells Per 1.08-mm^2 Field[a]

Control (normoxia)	62 ± 15 (*n* = 10)
Hypoxia	2322 ± 287(*n* = 25)*
Hypoxia + $NiCl_2$	235 ± 30 (*n* = 10)*
Hypoxia + pentobarbital	404 ± 55 (*n* = 21)*, **
Hypoxia + phenobarbital	745 ± 85 (*n* = 16)*

[a] Experiments in triplicate. Average ± SEM, *n* = total number of fields observed. *$P < 0.001$; **$P < 0.05$ versus hypoxia. Significance assessed by Dunn multiple-camparison nonparametric test versus control.

tubule cells (28). These channels are activated by protein kinase C agonists and respond to mechano-osmotic changes. Preliminary Northern blot and reverse transcriptase–polymerase chain reaction data that we have obtained support the concept that there is expression of a yet-to-be-identified Ca^{2+} channel in the renal cortex with low homology to the brain type Ni^{2+}-sensitive rbEII (BII) (31, 32) (data not shown).

Recent studies have shown that intercellular gap junction hemichannels, inhibited by gadolinium, are involved in the hypoxia-induced increase of intracellular calcium in proximal tubule cells (33). We have observed that changes in cell Ca^{2+} with hypoxia start focally in a few cells of the S2 segments and spread progressively to other cells of the same segment (Fig. 1). The change was prevented by $NiCl_2$, but it is unknown if it is the initiation or the spread of the calcium waves from cell to cell in hypoxic proximal S1-S2 segments that is Ni^{2+} sensitive.

Anoxia-Induced Cell Transport Changes. Reduced ability of proximal tubule cells to affect Na^+-gradient-dependent accumulation of AMG or of Pi after being exposed to anoxia and reoxygenation is likely a consequence of loss of the extra- to intracellular-Na^+ gradient caused by cell death, cell permeabilization, and reduced active extrusion of Na^+ in surviving cells. In addition, decreases in the surface-membrane abundance or activity of the respective co-transporters may contribute to this observation. Regardless of the cause, changes in cell transport were partially prevented by extracellular $NiCl_2$, suggesting that they were due, at least in part, to Ni^{2+}-sensitive processes such as those responsible for the rise in cytosolic $[Ca^{2+}]i$ and for cell permeabilization to PI. Much of the sodium-dependent uptake of AMG (80%) remains intact after a hypoxia-reoxygenation episode when the rise in cytosolic $[Ca^{2+}]i$ is blocked by $NiCl_2$. This indicates that in the presence of $NiCl_2$ the majority of the tubule cells survive the hypoxia and reoxygenation episode, and there is only a 20% irreversible reduction in their ability to accumulate AMG, probably related to cell death.

Hypoxia-Induced Cell Permeabilization. Hypoxia for 60 mins induced extensive cell permeabilization in PCTs, as assessed by nuclear PI staining. This was greatly attenuated when hypoxia occurred in the presence of 50 μM $NiCl_2$ (Fig. 3), which also prevented the rise in $[Ca^{2+}]I$. This finding is consistent with the previously described protective effect of BAPTA on hypoxic PCT cell death (9). It is thus possible that the cytoprotective effect of $NiCl_2$ may, at least in part, be due to inhibition of the rise in $[Ca^{2+}]I$. Because $NiCl_2$ does not have any effect on the aerobic uptake of Pi and AMG and promotes rather than interferes with recovery of Na-gradient-dependent uptakes of Pi and AMG after anoxia and reoxygenation, it is unlikely that it alters the extent of ATP depletion during hypoxia through inhibition of the Na^+-K^+-ATPase.

The protective effect of $NiCl_2$ is consistent with the preservation of microvillar and mitochondrial structure reported to occur in ATP-depleted PCTs when in the absence of extracellular Ca^{2+} (4). Nevertheless, in these fully ATP-depleted PCT cells, lactate dehydrogenase (LDH) release occurred even when incubated in Ca^{2+}-free medium indicating lethal damage to the cells. This Ca^{2+} independent injury could be prevented by glycine and alanine (4, 34). In our experiments, the presence of alanine in the incubation solutions may have minimized calcium independent cell damage (5). However, alanine alone did not prevent anoxia-induced cell permeabilization to PI: anoxic PCT cells preserved impermeability to PI only in the presence of $NiCl_2$. This suggests that permeabilization to PI in contrast to that to LDH depends on the anoxic increase in levels of cell Ca^{2+}. It is also possible that the degree of ATP depletion is more severe in PCTs treated with antimycin than in anoxia-exposed PCTs. In anoxia, anaerobic ATP sources such as glycolysis or anaerobic dismutations may be sufficient to sustain a minimum level of ATP required to maintain integrity of some PCT cell organelles (35) but were insufficient, even in the presence of alanine, to prevent cell permeabilization and nuclear staining with PI. Thus, hypoxic cell permeabilization to PI is nickel sensitive, alanine insensitive, and probably Ca^{2+} dependent.

The S3 segment has more glycolytic capacity and exhibits more intrinsic tolerance to *in vitro* hypoxia than do the nonglycolytic S1 and S2 segments (1, 2, 12). Consistent with this finding, we observed that in S3 segment cells there was no significant rise in cytosolic $[Ca^{2+}]I$ during 30 mins of hypoxia. This tubule segment has cells able to maintain sufficient extrusion of $[Ca^{2+}]i$ during hypoxia to match their Ca^{2+} entry, which may, in turn, be relatively slow. This cellular heterogeneity in the response of proximal tubule cells to hypoxia correlates with the "patchy" nature of proximal tubule injury observed during ischemia-reperfusion of the whole organ (36) and may reflect differences in glycolitic capacity and differences in the expression of $NiCl_2$-sensitive Ca^{2+} entry pathways in different proximal tubule segments.

In HEK cells, permeabilization to PI induced by hypoxia was reduced by $NiCl_2$, pentobarbital, and phenobarbital with relative effectiveness similar to the relative potencies they exhibit when used to inhibit Ca_v3 channels expressed in these cells (17, 37). This suggests that, at least in part, the $NiCl_2$-sensitive pathway responsible for hypoxia-induced cell permeabilization, involves such T-type calcium channels.

In summary, absence of $[Ca^{2+}]o$, or presence of $NiCl_2$ but not verapamil, prevents hypoxia-induced $[Ca^{2+}]I$ increase, cellular transport dysfunction, and cellular permeabilization to PI. These effects may involve a novel Ca^{2+} influx pathway with low homology to Ni^{2+}-sensitive rbIIE T-type channels.

We thank Dr. R. Faharani for all suggestions given. We acknowledge the assistance of Ms. B. Zavilowitz for her excellent technical contribution.

We thank Dr. M.S. Goligorsky, New York Medical College, for providing the HEK cells.

1. Ruegg CE, Mandel LJ. Bulk isolation of renal PCT and PST II. Differential responses to hypoxia. Am J Physiol 259(1, Pt 2):F176–F185, 1990.
2. Ruegg CE, Mandel LJ. Bulk isolation of renal PCT and PST I. Glucose-dependent metabolic differences. Am J Physiol 259(1, Pt 2):F164–F175, 1990.
3. Epstein FH, Balaban RS, Ross BD. Redox state of cytochrome aa3 in isolated perfused rat kidney. Am J Physiol 243:F356–F363, 1982.
4. Weinberg JM, Davis JA, Roeser NF, Venkatachalam MA. Role of increased cytosolic free calcium in the pathogenesis of rabbit proximal tubule cell injury and protection by glycine or acidosis. J Clin Invest 87:581–590, 1991.
5. Paller MS, Hoidal JR, Ferris TF. Oxygen free radicals in ischemic acute renal failure in the rat. J Clin Invest 74:1156–1164, 1984.
6. Weinberg JM, Davis JA, Abarzua M, Rajan T. Cytoprotective effects of glycine and glutathione against hypoxic injury to renal tubules. J Clin Invest 80:1446–1454, 1987.
7. Filipovic D, Sackin H. A Ca^{2+} permeable stretch activated cation channel in renal proximal tubule. Am J Physiol 260(1, Pt 2):F119–F129, 1991.
8. Morley P, Hogan MJ, Hakim AM. Calcium mediated mechanisms of ischemic injury and protection. Brain Pathol 4:37–47, 1994.
9. Kribben A, Wieder ED, Wetzels JF, Yu L, Gengaro PE, Burke TJ, Schrier RW. Evidence for role of cytosolic free calcium in hypoxia-induced proximal tubule injury. J Clin Invest 93:1922–1929, 1994.
10. Gupta RK, Dowd TL, Spitzer A, Barac-Nieto M. ^{23}Na, ^{19}F, l and ^{31}P multinuclear nuclear magnetic resonance studies of perfused rat kidney. Renal Physiol Biochem 12:144–160, 1989.
11. Tsien RW, Ellinor PT, Horne WA. Molecular diversity of voltage dependent calcium channels. Trends Pharmacol Sci 12:349–354, 1991.
12. Ruegg CE, Mandel LJ. Differential effects of hypoxia or mitochondrial inhibitors in renal proximal straight (PST) and convoluted (PCT) tubules (abstract). Kidney Int 37:529, 1990.
13. Schrier RW, Burke TJ. Role of calcium channel blockers in preventing acute and chronic renal failure. J Cardiovasc Pharmacol 18:S38–S43, 1991.
14. Yang JM, Lee CO, Windhager EE. Regulation of cytosolic free calcium in isolated perfused proximal tubules of Necturus. Am J Physiol 255(4, Pt 2):F787–F799, 1988.
15. Sanders JCJ, Isaacson LC. Patch clamp study of Ca^{2+} channels in isolated renal tubule segments. In: Pansu D, Bronner F, Eds. NATO ASI Series: Calcium transport and intracellular homeostasis. Berlin: Springer Verlag, Vol 48:pp27–34, 1990.
16. Hayashi K, Ozawa Y, Wakino S, Kanda T, Homma K, Takamatsu I, Tatematsu S, Saruta T. Cellular mechanism for mibefradil-induced vasodilation of renal microcirculation: studies in the isolated perfused hydronephrotic kidney. J Cardiovasc Pharmacol 42:697–702, 2003.
17. Lacinova L. Pharmacology of recombinant low-voltage activated calcium channels. Current Drug Target CNS Neurol Disord 3:105–111, 2004.
18. Chiu FC, Rozental R, Bassallo C, Lyman WD, Spray DC. Human fetal neurons in culture: intracellular communication and voltage- and ligand-gated responses. J Neurosci Res 38:687–697, 1994.
19. Rozental R, Mehler MF, Morales M, Andrade-Rozental MF, Kessler JA, Spray DC. Differentiation of hipoccampal progenitor cells in vitro: temporal expression of intracellular coupling and voltage- and ligand-gated responses. Dev Biol 167:350–362, 1995.
20. Grynkiewicz G, Poenie M, Tsien RY. A new generation of Ca^{2+} indicators with greatly improved fluorescence properties. J Biol Chem 260:3440–3450, 1985.
21. Kribben A, Wetzels JF, Wieder ED, Burke TJ, Schrier RW. New technique to assess hypoxia-induced cell injury in individual isolated renal tubules. Kidney Int. 43:464–469, 1993.
22. Todorovic SM, Jevtovic-Todorovic V, Mennerick S, Perez-Reyes E, Zorumski CF. Ca(v)3.2 channel is a molecular substrate for inhibition of T-type calcium currents in rat sensory neurons by nitrous oxide. Mol Pharmacol 60:603–610, 2001.
23. Flanagan RJ. Guidelines for the interpretation of analytical toxicology results and unit of measurement conversion factors. Ann Clin Biochem 35(Pt 2):261–267, 1998.
24. Sheridan AM, Schwartz JH, Kroshian VM, Tercyak AM, Laraia J, Masino S, Lieberthal W. Renal mouse proximal tubular cells are mouse susceptible than MDCK cells to chemical anoxia. Am Physiol Soc 265(3, Pt 2): F342–F350, 1993.
25. Jacobs WR, Sgambati M, Gomez G, Vilaro P, Higdon M, Bell PD, Mandel LJ. Role of cytosolic calcium in renal tubule damage induced by anoxia. Am J Physiol 260(3, Pt 1):C545–C554, 1991.
26. Constantinescu AR, Rozental R, Barac-Nieto M. Age dependence of tolerance to anoxia and changes in cytosolic calcium in rabbit renal proximal tubules. Pediatr Nephrol 10:606–612, 1996.
27. Kihara Y, Sasayama S, Inoko M, Morgan JP. Sodium calcium exchange modulates intracellular calcium overload during hypoxic reoxygenation in mammalian working myocardium. J Clin Invest 93:1275–1284, 1994.
28. Zhang MI, O'Neil RG. Molecular characterization of rabbit renal epithelial calcium channel. Biochem Biophys Res Commun 280:435–439, 2001.
29. Jan CR, Jiann BP, Lu YC, Chang HT, Huang JK. Effect of olvanil on cytosolic Ca^{2+} increase in renal tubular cells. Life Sci 71:3081–3090, 2002.
30. Yu ASL, Hebert SC, Brenner BM, Lytton J. Molecular characterization and nephron distribution of a family of transcripts encoding the pore-forming subunit of Ca^{2+} channels in the kidney. Proc Natl Acad Sci U S A 89:10494–10498, 1992.
31. Niidome TM, Kim S, Friedrich T, Mori Y. Molecular cloning and characterization of a novel calcium channel from rabbit brain. FEBS Lett 308:7–13, 1992.
32. Soong TW, Stea A, Hodson CD, Dubel SJ, Vincent SR, Snutch TP. Structure and functional expression of a member of the low voltage-activated calcium channel family. Science 260:1133–1136, 1993.
33. Vergara L, Bao X, Bello-Reuss E, Reuss L. Do connexin 43 gap-junctional hemichannels activate and cause cell damage during ATP depletion of renal-tubule cells? Acta Physiol Scand 179:33–38, 2003.
34. Frank A, Rauen U, de Groot H. Protection by glycine against hypoxic injury of rat hepatocytes: inhibition of ion fluxes through nonspecific leaks. J Hepatol 32:58–66, 2000.
35. Venkatachalam MA, Patel YJ, Kreisberg JI, Weinberg JM. Energy thresholds that determine membrane integrity and injury in a renal epithelial cell line (LLCPK1). Relationships to phospholipid degradation and unesterified fatty acid accumulation. J Clin Invest 81:745–758, 1988.
36. Kreisberg JI. Morphological factors. In: Brenner BB, Lazarus JM, Eds. Acute Renal Failure (2nd ed.). Livingstone, NY: Churchill, p45, 1985.
37. Todorovic SM, Perez-Reyes E, Lingle CJ. Anticonvulsants but not general anesthetics have differential blocking effects on different T-type current variants. Mol Pharmacol 58:98–108, 2000.